A&A 390, L19–L22 (2002)
DOI: 10.1051/0004-6361:20020893

Astronomy & Astrophysics

147 GHz VLBI observations: Detection of 3C 273 and 3C 279 on the 3100 km baseline Metsähovi – Pico Veleta

A. Greve[1], P. Könönen[2], D. A. Graham[3], K. Wiik[4,2], T. P. Krichbaum[3], J. Conway[5], F. Rantakyrö[6], S. Urpo[2], M. Grewing[1], R. S. Booth[5], J. A. Zensus[3], D. John[7], S. Navarro[7], A. Mujunen[2], J. Ritakari[2], J. Peltonen[2], P. Sjöman[2], E. Oinaskallio[2], and M. Berton[1]

[1] IRAM, 300 rue de la Piscine, 38406 St. Martin d'Hères, France
[2] Metsähovi Radio Observatory, Metsähovintie 114, 02540 Kylmälä, Finland
[3] Max–Planck–Institut für Radioastronomie, Auf dem Hügel 69, 53121 Bonn, Germany
[4] Tuorla Observatory, Väisäläintie 20, 21500 Piikkiö, Finland
[5] Onsala Space Observatory, 43920 Onsala, Sweden
[6] ESO, Casilla 19001, Santiago 19, Chile & Observatorio Cerro Calan, Universidad de Chile, Santiago, Chile
[7] IRAM, Nucleo Central, Avenida Divina Pastora 7, 18102 Granada, Spain

Received 8 April 2002 / Accepted 12 June 2002

Abstract. We report a successful VLBI observation at 147 GHz (2.1 mm) on the 3 100 km long baseline between the telescopes at Metsähovi (Finland) and Pico Veleta (Spain). The sources 3C 273B and 3C 279 were detected with a *SNR* of ∼10. For these sources we estimate that 25–30% of the total flux is detectable as correlated flux on the 3 100 km baseline, which gives at 147 GHz a lower limit of the brightness temperature of the inner VLBI jet region of $\sim 1\times10^{10}$ K.

Key words. mm VLBI – galaxies: quasars – galaxies: individual: 3C 273B, 3C 279

1. Introduction

Very Long Baseline Interferometry observations at millimeter wavelengths (3 mm–1 mm) provide the highest angular resolution, and therefore the possibility to explore the core regions of self–absorbed quasars and the origin of their jets. While VLBI at 86 GHz (3.5 mm) on intercontinental baselines has become a routine observing facility (CMVA, VLBA), VLBI observations at higher frequencies are still in an experimental state. So far, the only successful fringe detection was made at 223 GHz (1.3 mm) on the 845 km baseline (=0.65 × 10^9, $\lambda \equiv 0.65\,\mathrm{G}\lambda$) between Owens Valley and Kitt Peak [OVRO & KP, USA] (Padin et al. 1990) and at 215 GHz on the 1 147 km baseline (=0.88 Gλ) between the IRAM 30–m telescope at Pico Veleta [PV, Spain] and one antenna of the Plateau de Bure interferometer [PdB, France] (Greve et al. 1995; Krichbaum et al. 1997). These observations resulted in a marginal detection of 3C 273B on the OVRO–KP baseline and the detection on the PV–PdB baseline of several bright flat spectrum sources (including Sgr A*) with *SNR*s between 6 and 35. Since then, several VLBI experiments at 150 GHz (2 mm) and 230 GHz on intercontinental baselines were performed but did not reveal fringes, probably because of technical difficulties.

In this paper we report on a successful VLBI experiment at 147 GHz (2.1 mm) on the 3100 km long projected baseline (=1.5 Gλ) between the 14–m telescope at Metsähovi [MET, Finland] and the 30–m telescope at PV. A detection was not achieved, at the same time, on the approximately 3 to 4 times longer baseline between PV and SEST [Swedish–ESO Submillimetre Telescope, Chile] and MET and SEST, although SEST operated well during 86 GHz VLBI observations one day earlier. The experiment reported here was made, in particular, to explore the possibility of mm–VLBI at higher frequencies (∼150–230 GHz) and on moderately long baselines, as a preparatory step for future observations on intercontinental baselines.

2. Observations

2.1. Telescopes, receivers, T_{sys}

The observations were made in March (Day 79–81) and April (Day 99–101), 2001, with the IRAM 30–m telescope (at 2900 m altitude), the Metsähovi radome–enclosed 14–m telescope (at sealevel), and the SEST 15–m telescope (at 2500 m altitude). We counted on the possibility of low temperatures and low humidity in Finland in order to observe from the sealevel observatory MET at a low atmospheric attenuation (say, opacity $\tau(150\,\mathrm{GHz}) \lesssim 0.3$). The temperature was ∼–10° C in March and ∼–2° C in April.

At PV we used the 2 mm–SIS receiver, SSB–tuned with ∼13 dB rejection and 65 K receiver temperature.

Send offprint requests to: A. Greve, e-mail: greve@iram.fr

Table 1. Telescope characteristics at 150 GHz (2 mm).

Telescope	D (m)	Beam Width ($''$)	η	Gain Jy/K	T_{sys} (K)
Metsähovi	14	34	0.13	140	~ 1000
SEST	15	32	0.5	31	500
Pico Veleta	30	16	0.53	7.8	150–250

The beam width is measured at FWHP.
η is the aperture efficiency.

The chopper–wheel hot–cold–sky calibration was used which gives the system temperature (T_{sys}) and the atmospheric opacity (τ). A round–trip phase stability measurement was made by injecting a test signal into the stationary receiver located in the Nasmyth cabin. This test, which included the receiver, the IF chain, and the VLBI terminal, indicated that the noise of the round–trip phase did not exceed ~45° (peak-to-peak). A part of the phase noise (at PV, MET, and SEST) is due to the test signal and not the actual VLBI system. The characteristics of the 30 m telescope at 150 GHz at the time of observation are given in Table 1.

The Metsähovi telescope had not been used before at 150 GHz. The observations were made with the first–generation IRAM 2 mm–SIS receiver installed on this telescope, SSB–tuned with a rejection of ~8 dB. The receiver temperature was ~200 K; a direct determination of T_{sys} was not possible. For the time of observation we derived from the meteorological data the opacity $\tau(150\,\mathrm{GHz}) \approx 0.5$–$0.9$ at the 20–30° elevation range of the primary sources (Fig. 1), and we estimate $T_{sys} \approx 1000$ K. A round–trip phase stability measurement was made by injecting a test signal into the receiver while the telescope was pointing towards horizon. This test, including the receiver, the IF chain, and the VLBI terminal, indicated that the noise of the round–trip phase did not exceed ~50° (peak-to-peak), similar to the value measured at PV. A phase test at the ~25° higher elevation of the primary sources (Fig. 1) was not possible. The characteristics of the Metsähovi telescope at 150 GHz at the time of observation are given in Table 1.

At SEST we used the 2 mm–SIS receiver, SSB–tuned with a rejection of ~15 dB and a receiver temperature of ~200 K. The measured T_{sys} was ~500 K. A round–trip phase stability measurement was made by injecting a test signal into the receiver while the telescope was pointing towards horizon. This test, including the receiver, the IF chain, and the VLBI terminal, indicated noise of the round–trip phase of ~90° (rms), or more. A phase test at the higher elevation of the sources was not possible. The preceeding 86 GHz VLBI observations used a phase–locked fundamental mode oscillator and phase–locked multipliers to generate the corresponding LO frequency. For the 147 GHz VLBI observations we used a phase–locked synthesizer and multipliers. We have been aware of several shortcomings in this LO generation and in addition of the possibility of considerable phase noise of the maser signal. Improvements in the phase stability of the system are currently in progress. The characteristics of the SEST telescope at 150 GHz at the time of observation are given in Table 1. SEST reported unfavourable meteorological conditions (clouds, high humidity), which certainly has contributed to the non–detection at 2 mm wavelengths on the long baseline towards SEST.

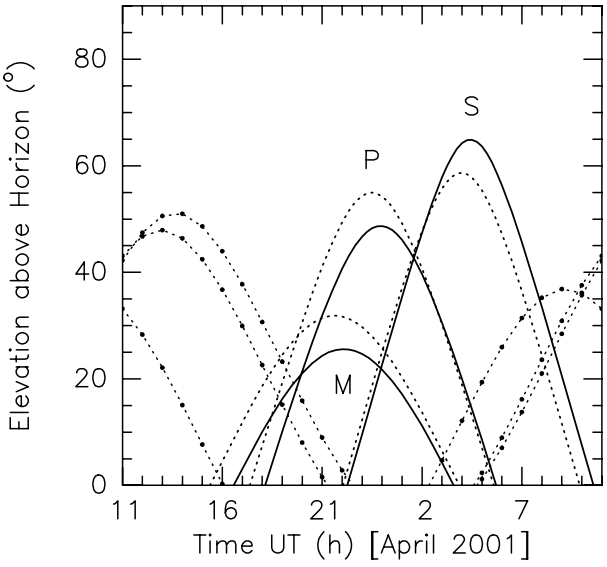

Fig. 1. Common visibility of 3C 279 (full line) and 3C 273B (dashed line) at Metsähovi (M), Pico Veleta (P), and SEST (S). For a common visibility between MET–PV–SEST the elevation of the sources is not higher than 25° elevation. The lines with dots show the position of the planets (from left to right: Venus, Saturn, Jupiter) as seen at Metsähovi and used for pointing.

Although we had selected for observation several bright 3 mm VLBI sources, the emphasis was placed on the strongest (single–dish flux density) sources 3C 273B and 3C 279, which culminate at MET at 25° and 30° elevation (Fig. 1). At MET, pointing was made by using the general pointing model and corrections for the 147 GHz observations determined from the planets Venus, Jupiter, and Saturn, of which the latter two were at the beginning of the VLBI observations in elevation close to 3C 273B and 3C 279 as shown in Fig. 1 (reducing instabilities of the receiver liquid He cooling system when rapidly tilting the telescope; earlier on the 30–m telescope the receiver was used only in horizontal position). The pointing on these QSOs was probably accurate to within ±5″. For the other QSOs (Sect. 2.3) blind pointing was applied with perhaps significantly larger uncertainties for larger elevation distances from the planets. SEST used the pointing model biweekly determined from SiO masers (86 GHz); the pointing accuracy over the whole sky was typically 3″ rms in azimuth and elevation direction. At PV we used interlaced scans across the sources which provide a pointing accuracy within ±2″ in azimuth and elevation direction.

2.2. VLBI recording, correlation

The observations at MET and PV were made at Left-Circular-Polarization, SEST used Linear Polarization. A few observations with a 90°–rotated polarizer (PV) gave correlations with marginal *SNR*s of 5.8–6.5 (baseline 1630–1760 km), although lower values were expected in case of clean polarization. This condition may not have been realized with the IRAM provided

Table 2. Measured single–dish flux densities (S) in April/March 2001 (PV).

Source	S (86 GHz) [Jy]	S (147 GHz) [Jy]	S (230 GHz)	α_{86}^{230}
3C 273B	12.5 ± 0.6	6.6 ± 0.8	5.35 ± 0.7	–0.87
3C 279	20.6 ± 0.4	13.4 ± 0.65	10.2 ± 1.1	–0.72

classical design square groove polarizer used at MET. The data were recorded in MK IV mode at a rate of 256 Mbit/s and 1 bit sampling. 16 channels (8 USB, 8 LSB) of 8 MHz bandwith each were recorded at PV, MET, and SEST. This mode of observation allowed 6.5 min continuous recording with a total bandwidth of 128 MHz, using thick tapes at MET and SEST and thin tapes at PV. The observations of 3C 273B and 3C 279 were closely packed during the time of culmination at MET and the common visibility (Fig. 1). The data were correlated at the MPIfR–Bonn, using the standard software for MK IV VLBI data.

2.3. Observed sources

Although we concentrated on the observation of 3C 273B and 3C 279 with presently the highest 2 mm flux density, we also observed the QSOs 0133+476, 0234+285, 0336–019, 0420–014, 0727–115, 1730–130 (NRAO530) [11], 1749+096 (OT081) [11], 1921–293 (OV236) [7], 2145+067 [7], 2223–052, 3C 111, 3C 345, 3C 454.3, 4C 39.25. These sources have relatively high single–dish flux densities (~5 Jy range), and several of them were selected because of their previous detection at 215 GHz on the PV–PdB baseline (measured *SNR* in square brackets) (Greve et al. 1995; Krichbaum et al. 1997). Except 3C 273B and 3C 279, none of the sources was detected.

2.4. Single–dish flux densities

Table 2 gives for 3C 273B and 3C 279 the observed single–dish flux densities (S) and the spectral index α_{86}^{230} between 86 GHz and 230 GHz ($S = \nu^{\alpha}$) at the time of observation. The 86 GHz data are derived from calibrated pointing scans made with the IRAM 30–m telescope during the immediately preceeding 3 mm CMVA VLBI observations; from the IRAM 30–m archive we took the data at 230 GHz which were obtained from calibrated pointing scans made on April, 17 and 30, 2001 (U. Lisenfeld, priv. comm.). With respect to a straight–line fit $\log S = \alpha \log \nu$ we notice that the flux density S (147 GHz) of 3C 273B is probably 15–20% too low, for 3C 279 the flux density is probably ~5% too low.

3. Result

On the 1630 km to 3100 km long projected baseline between Metsähovi and Pico Veleta we have detected the sources 3C 273B and 3C 279, in March and April, 2001, and on consecutive days, with a *SNR* of up to 10, as shown in Fig. 2. We note that the highest *SNR* occured near the largest

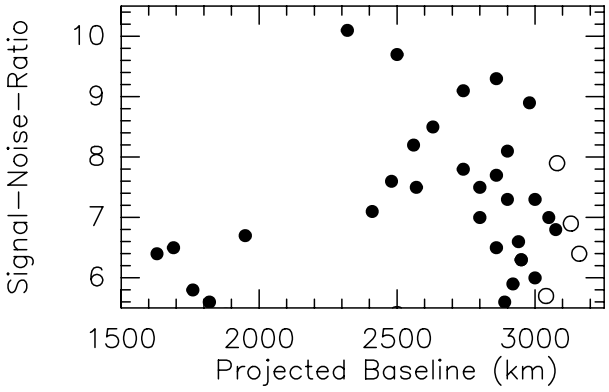

Fig. 2. *SNR* of the detection of 3C 279 (dots) and 3C 273B (open circles) as function of the projected baseline between PV and MET. The short projected baselines correspond also to a low elevation of the sources at MET and PV. Observations of March and April, 2001.

projected *uv*–spacing of ~2800 km length, i.e. 1.3 Gλ. We cannot exclude that changing atmospheric conditions are at least in part responsible for the observed variations of the *SNR* and by this also of the variation of the correlated flux density versus the projected baseline length. However for 3C279, where most of the detections are obtained, we can also simulate the variation of the *SNR* as seen in Fig. 2 if we assume a double structure ($\Delta r \simeq 0.3$ mas) of two Gaussian components (flux ratio 1.2) aligned at the position angle of the known VLBI jet (PA = –137°, Wehrle et al. 2001). Due to the limited amount of data, a detailed modelling of the underlying brightness distribution is not possible. We conclude therefore that the observed variation of the *SNR* with *uv*–distance nevertheless is in good agreement with the expected beating of the visibility, if the source structure of 3C279 resembles somehow the VLBI jet structure seen earlier and at longer wavelengths. Thus it is possible that 3C 279 consists also at 147 GHz of several (at least two) compact (*FWHM* < 0.2 mas) components which are separated from each other on the 0.1–0.3 mas scale.

The detections were favoured by stable atmospheric conditions at both sites (MET, PV), which made it possible to integrate over the full scan length of 6.5 min. For a typical scan of 6.5 min length we show in Fig. 3 the phase and amplitude stability measured at 147 GHz on 3C 279. The data are binned into 10 s and 30 s time intervals. Using the parameters of Table 1, on the 1.3 Gλ baseline the detected correlated flux density of 3C 279 is $F \approx 3.5 \pm 0.5$ Jy (Fig. 3). For 3C 273B we find in a similar way $F \approx 2.2 \pm 0.7$ Jy. The error is primarily due to the uncertainties in the gain and $T_{\rm sys}$ of the MET telescope. In view of the uncertainties in the calibration, and of a possible polarization mismatch which may have introduced additional noise (square grooves prone to reflections and standing waves), the derived correlated flux densities and F/S ratios (Table 3) are probably lower limits.

The detection of *SNR* ≈ 8–10 is consistent with the telescope performances and the derived correlated flux density (F [Jy]) of 3C 273B and 3C 279. For coherent integrations between 30 and 60 s in lengths the correlation amplitudes are approximately constant, while for shorter times the apparent amplitudes increase due to noise. The amplitudes for a full 360 s

Table 3. Correlated flux densities (F) and ratios F/S, at 147 GHz.

Source	F(147 GHz) [Jy] (2001)	F/S (147 GHz) (2001)	F/S (86 GHz)[a] (1995)	F/S (215 GHz)[a] (1995)
3C 273B	2.2 ± 0.7	$30 \pm 10\%$	$28 \pm 10\%$	$6 \pm 2\%$
3C 279	3.5 ± 0.5	$25 \pm 5\%$	$80 \pm 5\%$	$30 \pm 3\%$

[a] obtained in the VLBI experiment PV–PdB, 1995.

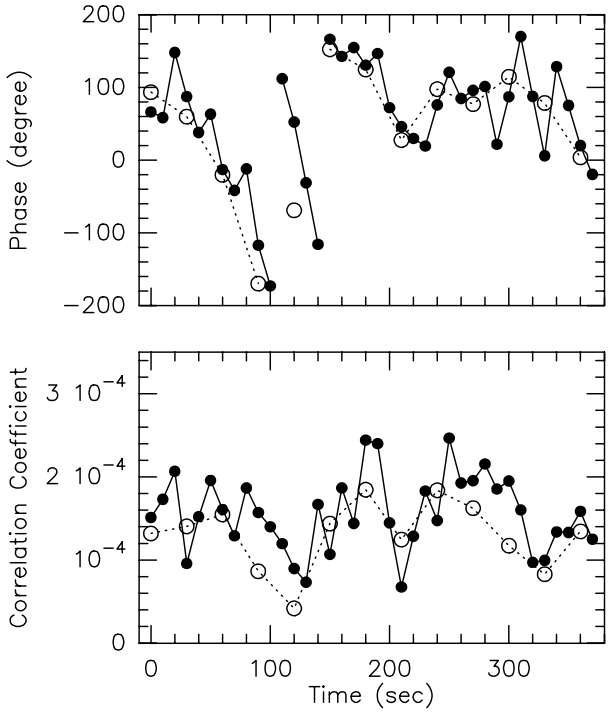

Fig. 3. Phase stability and correlation coefficient measured at 147 GHz on the MET–PV baseline, source: 3C 279. Solid dots: averages for 10 s time intervals, open circles: averages for 30 s time intervals; same scan of 6.5 min length. Date: 2001, day 81, 00:20 UT.

coherent integration are typically 0.7 of the 60 s value, while the *SNR* scarcely increases for integrations longer than 100 s. When using the relation (Rogers et al. 1984) between the *SNR*, the telescope efficiencies (ηA, A = aperture area [m^2]), the receiver and sky quality ($T_{\rm sys}$ [K]), and the recording ($\Delta\nu$ = bandwidth [Hz]) and correlation (τ = integration time [s]) characteristics, i.e.

$$SNR \approx L \sqrt{2\,(\eta A)_1(\eta A)_2\,\tau\Delta\nu/T_{\rm sys,1}T_{\rm sys,2}} \times (F/2k) \qquad (1)$$

(L = correlation efficiency ≈ 0.64, k = Boltzmann constant = $1.38{\times}10^{-23}$ WK^{-1}) we obtain for $SNR = 10$, $\tau = 30$ s, $\Delta\nu = 128$ MHz, and the parameters of Table 1, the correlated flux density $F \approx 2$–3 Jy.

Table 3 summarizes the result. We find that the ratio of the correlated flux density (F) and the single–dish flux density (S) is approximately 25–30% for both sources. The table gives also the ratios F/S measured at 86 GHz and 215 GHz in the 1995 VLBI experiment between PV and PdB. For both sources, the relatively large difference of the 147 GHz F/S ratios with respect to those measured at 86 GHz and/or 215 GHz indicates considerable substructure on sub–mas scales or structural variability between 1995 and 2001.

At the longest baseline of $B \approx 3100$ km, the angular resolution is $\theta \approx \lambda/B \approx 0.14$ mas. Figure 2 suggests that the sources 3C 279 and 3C 273B are barely resolved and hence that the size of their cores (if we assume a single Gaussian–type source) is $\theta_{\rm S} \lesssim \theta$. Using as *upper* limit $\theta_{\rm S} = 0.14$ mas in the relation of the brightness temperature

$$T_{\rm B} = 1.22\,F/(\nu\,\theta_{\rm s})^2 \qquad (2)$$

(with $T_{\rm B}$ in K/10^{12}, F in Jy, ν in GHz, and $\theta_{\rm S}$ in mas), we obtain as *lower* limit of the brightness temperature $\sim 1{\times}10^{10}$ K $\lesssim T_{\rm B}$ for $F \approx 2$–3 Jy. Unless consisting of much smaller components, our observation may indicate that at 2.1 mm wavelength these sources apparently do not reach a brightness temperature of $\sim 10^{11}$ K as observed at 86 GHz in the core of compact VLBI sources (Lobanov et al. 2000). However, with respect to the uncertainty in the amplitude calibration and the source structure, a higher brightness temperature cannot be ruled out.

At present, the resolution $\theta \approx \lambda/B$ (B = baseline) $\approx 140\,\mu$as and the field of view $\Theta \approx \lambda/B\,(\nu/\Delta\nu) \approx 160$ mas of the reported 2 mm VLBI observation on the 3100 km long baseline between MET–PV is of similar order as the resolution and field of view of 3 mm VLBI observations on a $B = 5000$ km intercontinental baseline. 2 mm VLBI observations on intercontinental baselines (5000 km or longer) should therefore be tried for even higher angular resolution.

Acknowledgements. We appreciated the efficient engineering support from B. Lazareff, J.–Y. Chenu, S. Sanchez, J. Peñalver (IRAM), Lars G. Gunnarsson (Onsala), and M. Anciaux (SEST). F. Mattiocco (IRAM) measured the LCP–plates and by this clarified some uncertainties. We also thank the colleagues at the observatories and the correlator for their support; and C. Thum (IRAM) and L.-A. Nyman (SEST) for easy scheduling of the observations. We thank the referee, J. Ulvestad, for his comments which helped substantially to improve this publication.

References

Greve, A., Torres, M., Wink, J. E., et al. 1995, A&A, 299, L 33
Krichbaum, T. P., Graham, D. A., Greve, A., et al. 1997, A&A, 323, L 17
Lobanov, A. P., Krichbaum, T. P., Graham, D. A., et al. 2000, A&A, 364, 391
Padin, S., Woody, D. P., Hodges, M. W., et al. 1990, ApJ, 360, L 11
Rogers, A. E. E., Moffet, A. T., Backer, D. C., & Moran, J. M. 1984, Radio Sci. 19, 1552
Wehrle, A. E., Piner, B. G., Unwin, S. C., et al. 2001, ApJS, 133, 297